Elastic excitations in BaTiO₃ single crystals and ceramics: Mobile domain boundaries and polar nanoregions observed by resonant ultrasonic spectroscopy

Ekhard K. H. Salje,[2,*] Michael A. Carpenter,[2] Guillaume F. Nataf,[1,2] Gunnar Picht,[3] Kyle Webber,[3]
Jeevaka Weerasinghe,[4,5] S. Lisenkov,[6] and L. Bellaiche[4]

[1]*Department of Earth Sciences, Cambridge University, Cambridge CB2 3EQ, UK*
[2]*Grenoble Institute of Technology, 46 Avenue Félix-Viallet Grenoble, France*
[3]*Institute for Ceramics in Mechanical Engineering, Karlsruhe Institute of Technology, Haid-Und-Neu-Straße 7, D 76131 Karlsruhe, Germany*
[4]*Department of Physics and Institute for Nanoscience and Engineering, University of Arkansas, Fayetteville, Arkansas 72701, USA*
[5]*Department of Physics, University of North Texas, Denton, Texas 76205, USA*
[6]*Department of Physics, University of South Florida, Tampa, Florida 33620, USA*

The dynamic properties of elastic domain walls in BaTiO₃ were investigated using resonance ultrasonic spectroscopy (RUS). The sequence of phase transitions is characterized by minima in the temperature dependence of RUS resonance frequencies and changes in Q factors (resonance damping). Damping is related to the friction of mobile twin boundaries (90° ferroelectric walls) and distorted polar nanoregions (PNRs) in the cubic phase. Damping is largest in the tetragonal phase of ceramic materials but very low in single crystals. Damping is also small in the low-temperature phases of the ceramic sample and slightly increases with decreasing temperature in the single crystal. The phase angle between the real and imaginary part of the dynamic response function changes drastically in the cubic and tetragonal phases and remains constant in the orthorhombic phase. Other phases show a moderate dependence of the phase angle on temperature showing systematic changes of twin microstructures. Mobile twin boundaries (or sections of twin boundaries such as kinks inside twin walls) contribute strongly to the energy dissipation of the forced oscillation while the reduction in effective modulus due to relaxing twin domains is weak. Single crystals and ceramics show strong precursor softening in the cubic phase related to polar nanoregions (PNRs). The effective modulus decreases when the transition point of the cubic-tetragonal transformation is approached from above. The precursor softening follows temperature dependence very similar to recent results from Brillouin scattering. Between the Burns temperature ($\approx$586 K) and T_c at 405 K, we found a good fit of the squared RUS frequency [$\sim \Delta (C_{11} - C_{12})$] to a Vogel–Fulcher process with an activation energy of $\sim$0.2 eV. Finally, some first-principles-based effective Hamiltonian computations were carried out in BaTiO₃ single domains to explain some of these observations in terms of the dynamics of the soft mode and central mode.

I. INTRODUCTION

The elastic properties and the precursor, relaxor-type behavior of BaTiO₃ have been investigated in great detail over several decades.[1–7] BaTiO₃ is a classic ferroelectric and ferroelastic material, which undergoes successive structural phase transitions from cubic ($Pm\bar{3}m$) to tetragonal ($P4mm$) at $T_{C\text{-}T}$, tetragonal to orthorhombic ($Amm2$) at $T_{T\text{-}O}$, and orthorhombic to rhombohedral ($R3m$) at $T_{O\text{-}R}$.[8] Bulk properties are well known, but it has been shown more recently that, by careful preparation of domain structures (domain engineering), one can obtain very high piezoelectric responses,[9–13] which go well beyond values expected from the bulk. It became also clear that nanostructured BaTiO₃ shows colossal dielectric responses.[14] The interfacial effects, such as grain boundaries and twin boundaries, were then shown to depend strongly on the chemical compositions of the samples.[15] Finally, twinning remained visible for nanocrystals of sizes well below 100 nm[16] so that it is not possible to correlate the nanoscale behavior of BaTiO₃ simply with the intrinsic bulk behavior modified by the surfaces[17] because mobile twin boundaries persist to the smallest-known grain size and modify the macroscopic behavior of the sample significantly.

The question arises, therefore, whether the enhanced polar properties are solely a matter of engineered domain structures or whether the increased density of domain boundaries between domains plays an additional role. This means that we need to assess the importance of "domain engineering" compared with "domain boundary engineering", which attempts to modify domain boundaries sufficiently to lead to similar enhancement effects.[18–28] The direct comparison of static properties is at the limit of our experimental facilities (e.g. Ref. 24) and has not previously been undertaken in BaTiO₃. A similar route was taken by Hlinka *et al.*[29] who used Landau–Ginzburg modeling to explore the properties of the twin boundaries and compared the results with experimental observations. The observation of largely enhanced piezoelectricity by application of electric fields along specific directions in ferroelectric crystals, which frustrate the movement of twin walls,[11] requires that domain structures become extremely fine. Hlinka *et al.*[29] argued that it might then be possible to detect intrinsic piezo-effects from the domain walls themselves. They analyzed the intrinsic domain structure using a Landau–Ginzburg approach and found some enhancement of the piezoelectric coefficients for domain thicknesses below 50 nm, although the effect was much smaller than that observed experimentally.[11]

Other physical mechanisms that could lead to a high piezoelectric response include the accumulation of point defects in domain walls and dynamic features, such as the

formation of latches and kinks in domain walls, which could be mobile under electric fields even when the straight segments of the walls are not. Such effects were seen in other materials[24] found by computer simulations.[17]

It is the purpose of this paper to show, first, results of dynamic measurements of elastic properties using the resonant ultrasonic spectroscopy (RUS) technique. This experimental technique operates at frequencies between 0.05 and 1.2 MHz and detects only those resonances which are related to elastic deformations. The low amplitude of the resonance compared with the more commonly used dynamic mechanical analysis (DMA) technique excludes influences from large domain wall movements.[24] Local excitations of twin walls ($90°$ boundaries but not $180°$ boundaries in $BaTiO_3$) and polar nanodomains related to small volume changes are visible using this technique. We will then show that the RUS results are compatible with first principles calculations which show the trends in the temperature evolution of the central mode ($\sim$Ti flipping mode) to be the source of the changes in phase angle of the RUS signal.

II. RUS METHODOLOGY

We briefly summarize some of the key points of RUS in systems with mobile domain boundaries. Resonant ultrasonic spectroscopy spectra are characterized by three parameters, namely the resonance frequency, the amplitude, and the phase shift.[30,31] We are less interested in their absolute values but in the dependence of these parameters on the external control parameters of the experiment (e.g. temperature, strain, electric fields). Resonant ultrasonic spectroscopy signals are not local resonances but represent the vibration of the sample and the attached RUS equipment (sample rods and transducers). In an RUS experiment, the driving transducer leads to sustained vibrations of the sample (the "ringing" of the sample), with an amplitude which is detected by the receiver transducer. The complex amplitude is given by a sum of oscillators (or some other combination reflecting the effective medium of the sample):

$$x(\omega,t) = \sum \left\{ A_i A_{\text{excitation}} / \left[\omega_i^2 - \omega^2 + i\omega_i\omega/Q \right] \right\} \times \exp(-i\omega t + \varphi),$$

where $A_{\text{excitation}}$ is the amplitude of the forcing excitation, ω_i is the singular frequency at which the sample would ring if there were no damping ($1/Q \to 0$). The complex amplitude can be split into the real part and the imaginary part. Both trajectories are displayed in the complex plane as Cole–Cole plots (or Nyquist plots),[32] whereby each resonance displays a circle through the origin. The circle is rotated by the phase φ around the origin. More complex trajectories, including the superposition of several circles, relate to interacting resonances. The initial phase factor of an RUS resonance depends on the geometrical coupling between the transducers and the sample. When the control parameter is changed, resonances and excitations in the RUS frequency range will change the phase factor, which is seen as a rotation of the resonance circle around the origin. If several resonances couple, the phase factors also couple and lead to a complex spiral web of curves which cannot be allocated to single-mode excitations of the sample. The

change of phase with the control parameter has a real physical meaning such as nonlinear damping of the oscillation or a multitude of resonance modes, which are spatially separated but very similar in frequency. Another mechanism relates to threshold behavior of domain movement, e.g. when the driving force needs to exceed a value to produce a sudden advance of the domain boundary.[18,33] One expects no change of the RUS phase if a sample has a stable microstructure, which does not depend on the control parameter.[34–37] This is born out in quartz where RUS phase angles are virtually independent of temperature.[38] In $BaTiO_3$, we find the same situation in the orthorhombic phase. If dynamic microstructures, such as jerky propagation occur, they will change the phase angle if the time delay and the resonance frequency are of similar order of magnitude.[17] Changing viscous behavior will influence the phase angle even if the effect on Q is too small to be observed.

In this paper, we are not interested in the absolute values of the elastic moduli (see Ref. 34). Instead, we wish to determine their relative changes due to phase transitions. The scaling of the moduli is related to the resonance frequency

$$\Delta f^2 \sim C^*,$$

where C^* is the relevant effective elastic modulus or combination of moduli of the sample. The modulus will change during the phase transition whereby the intrinsic change is irrespective of the domain formation.[35] Twin boundaries have two effects on C^* (e.g. Ref. 29). First, any twin boundary leads to a shear of the adjacent domains so that the projection of the elastic modulus along the wave vector of the vibration is generally changed. Twin angles ω are small so that the effect of the domain shear is also small [$\cos^2(\omega) \lesssim 1$]. The second effect occurs when domain boundaries are mobile. They reduce the effective modulus of the sample, and their friction increases the damping of the RUS resonance.[36] This effect is the same, albeit at higher frequencies, as in DMA experiments, and we refer the reader to DMA literature for further analysis of the moving twin walls on the resonance frequency.[36] The effect is sometimes referred to as "visco-elastic" because the response is no longer purely elastic.

The damping is described by reductions of the quality factor Q and is directly related to the energy loss, e.g. due to friction of the moving walls. Friction relates to the effective medium behavior of the sample and is not directly related to an individual wall movement. In particular, wall friction does not necessarily reflect the propagation of walls with constant wave number but will often refer to jerky (or stepwise) propagation, which is perceived over larger time scales as "smooth" movement.[17] It is not possible to distinguish between these very different mechanisms by measurements of $Q(\omega)$. A simple model to understand the effect of visco-elasticity is to consider a visco-elastic layer attached to a loss-free resonator.[37]

The phase angle generally changes with decreasing Q. The line shape of the resonance function is also modified. Explicit calculations of the change in thickness vibrations of quartz and $BaTiO_3$ for viscoelastic impurities[38] have found Q values of $BaTiO_3$ near 10^3, a value much smaller than quartz but still much larger than the value we will report in this paper for moving twin walls. The effect of microstructural relaxations over long time spans was reported in Ref. 39.
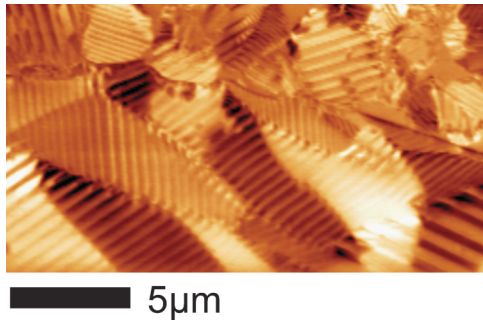
FIG. 1. (Color online) Microstructure of a heavily twinned BaTiO$_3$ ceramic at room temperature.

III. EXPERIMENTAL

Two samples of BaTiO$_3$ were analyzed using RUS equipment described elsewhere.[40] In the He flow cryostat, the samples were mounted across faces directly between the transducers. In the high-temperature system, they were mounted across pairs of corners between the tips of alumina rods, which protruded into a resistance furnace. In this case, the transducers were at the other ends of the rods, outside the furnace. The single crystal was in the form of an imperfect rectangular parallelepiped with mass 0.5649 g and dimensions ~7.040 × 4.089 × 3.457 mm^3. The ceramic sample[41] was a rectangular parallelepiped with mass 0.3105 g and dimensions 4.193 × 3.777 × 3.287 mm^3. Each spectrum, between 0.1 and 1.2 MHz, contained 65 000 data points, with the exception of high-temperature spectra from the ceramic sample, which contained 50 000 data points. Each grain in this sample is heavily twinned (Fig. 1). Data were collected in heating and cooling sequences, as set out in Table I, with a settle time of 15 mines to allow thermal equilibration at each temperature. Spectra were analyzed using the IGOR (WaveMetrics) software package. In particular, the data were analyzed for the frequency shift of selected sharp lines with little overlap with adjacent resonances. The Nyquist plots were restricted to small frequency intervals near the resonance to that each resonance allowed one circle with little overlap with other resonances.

TABLE I. Experimental conditions for RU measurements. For single crystals, low-T data were collected before the high-T data. For ceramics, the high-T data were collected first.

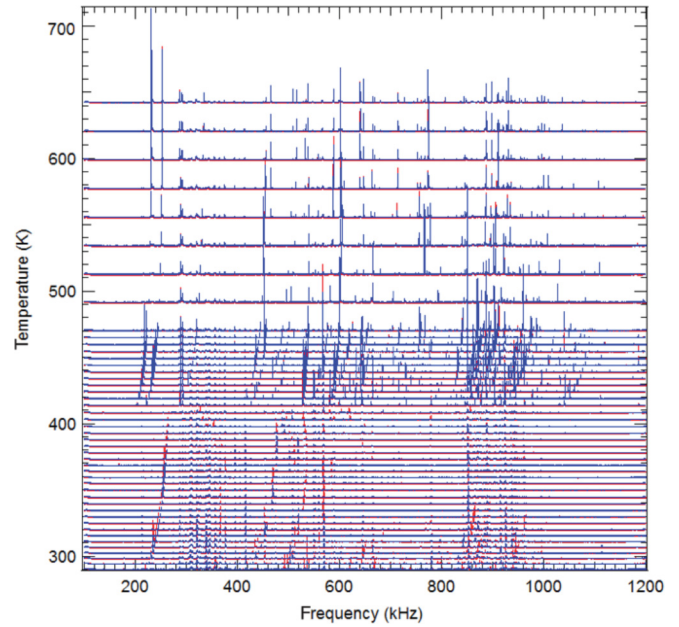|	LT sequences (K)	Step (K)	HT sequences (K)	Step (K)
Single crystal	305–270	1	295–480	5
	270–210	5	480–640	20
	210–180	1	640–480	20
	180–10	5	480–295	5
	180–210	1		
Ceramic	280–10	30	293–693	30
	10–250	5	693–293	5
	250–310	2		
	310–250	2		

FIG. 2. (Color online) Stack of RUS spectra for a single crystal of BaTiO$_3$ collected during heating and cooling from 295 to 640 K. The y axis is amplitude. The individual spectra have been displaced in proportion to the temperature at which they were collected, and the axis label is shown as temperature. Weak peaks, which do not vary with temperature, are from alumina rods of the high-temperature instrument.

IV. RESULTS

A typical stack of spectra from the single crystal is shown in Fig. 2. The temperature dependence of the squared frequency (∝ elastic moduli) and the inverse quality factor Q^{-1} are shown in Fig. 3. The stability field of the cubic phase is characterized
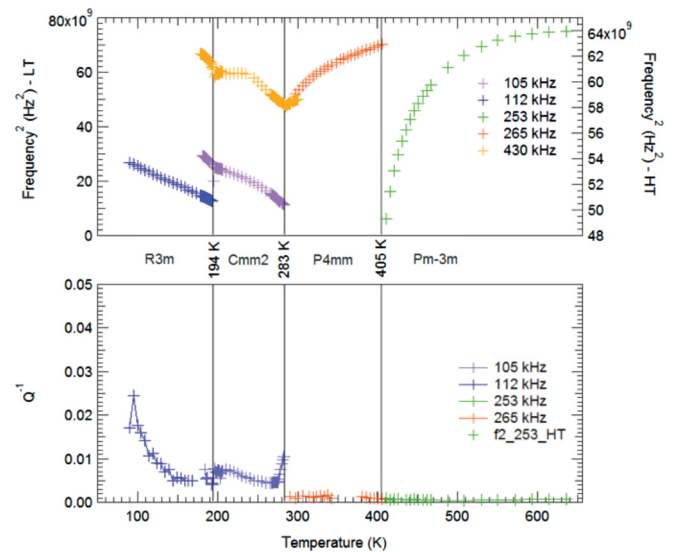

FIG. 3. (Color online) Squared frequency and inverse quality factor for a single crystal of BaTiO$_3$. The phase transition points correspond to local minima of the RUS resonance frequency. The experimentally observed transition temperatures are 405, 283, and 194 K.

by very low values of Q^{-1} and precursor softening as $T \to T_{CT}$ from above. The cubic $\leftrightarrow$ tetragonal transition is marked by a local minimum in f^2 at $T_{CT} = 405 \pm 1$ K. The tetragonal phase presents the same pattern of softening with falling temperature and low values of Q^{-1}. It was not possible to obtain good fits of the resonances between 343 and 380 K because of noise from alumina rods of the high-temperature instrument which submerged the sample signal, as shown in Figs. 2 and 3. This does not indicate high damping of the sample, however. The tetragonal $\leftrightarrow$ orthorhombic transition relates to the softening and then stiffening of the elastic constant with falling temperature with a minimum at $T_{TO} = 283 \pm 1$ K. A weak increase of Q^{-1} in the orthorhombic phase occurs near T_{TO}. The orthorhombic $\leftrightarrow$ rhombohedral transition shows a minimum in f^2 at $T_{OR} = 194 \pm 1$ K. The elastic constant stiffened in the rhombohedral phase with falling temperature. A broad Debye-like peak in Q^{-1} occurs in the stability field of the rhombohedral phase with a maximum at 95 K.

The results for the ceramic sample are similar to those of the single crystal with some systematic deviations (Figs. 4 and 5). In the stability field of the cubic phase, the elastic constants again first stiffened and then softened with decreasing temperature. The effect is larger than in the single crystal. The maximum of the resonance frequency occurs near $T_B = 586 \pm 1$ K. The values of Q^{-1} are low, indicating low dissipation. The cubic $\to$ tetragonal transition is then marked by the complete disappearance of peaks from the resonance spectra at $T_{CT} = 405$ K as shown in Fig. 5. This is the key difference between the spectra obtained from single crystals and those of ceramics:
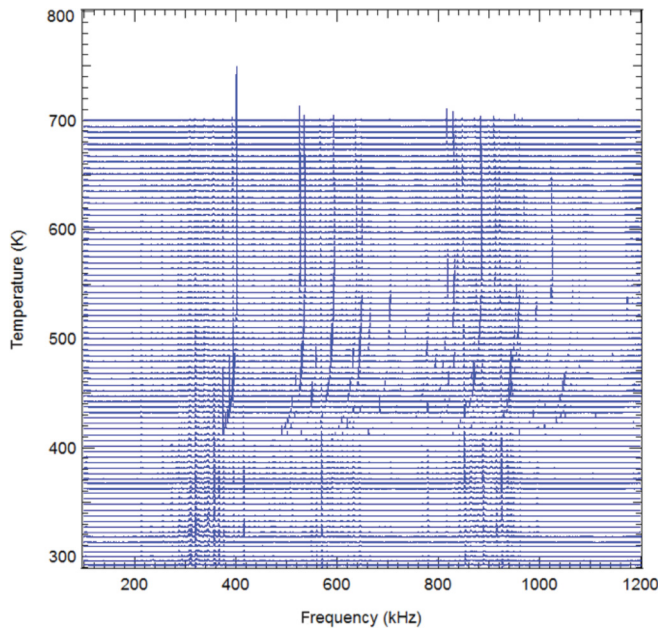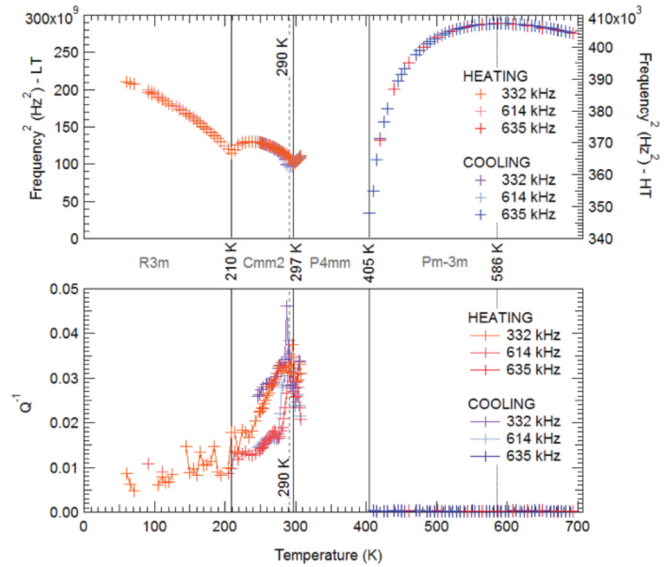

FIG. 5. (Color online) Squared frequency and inverse quality factor of BaTiO$_3$ ceramic. The phase transition points are shown by local minima of the temperature evolution of the RUS resonance frequency. The experimentally observed transition temperatures are 405, 297, and 210 K. Note the high values of Q^{-1} (damping) in the tetragonal and orthorhombic phases.

The single crystal shows the "normal" temperature behavior of a resonating tetragonal phase, while the ceramic absorbs most injected energy and does not ring. At lower temperatures, it was possible to find resonances in the stability field of the tetragonal phase, near 300 K, with high damping. These resonances could be detected because of the much better signal-to-noise ratio of spectra using the low-temperature instrument. The tetragonal $\leftrightarrow$ orthorhombic transition is marked by a stiffening of the elastic constant with falling temperature at $T_{TO} = 290 \pm 1$ K. On heating, this transition is shifted to 297 ± 1 K, showing a thermal hysteresis of 7 K. Near the transition, we find a steep increase in Q^{-1} a few Kelvin below the transition point. The orthorhombic $\leftrightarrow$ rhombohedral transition corresponds to a minimum in f^2 at $T_{OR} = 210 \pm 1$ K. Here, Q^{-1} is relatively low (~ 0.01) in the stability field of the rhombohedral phase.

We now compare the Nyquist diagrams of the various phases. In Fig. 6, we plot the diagrams for the single crystal and, in Fig. 7, for the ceramic sample. In the ceramic sample, Nyquist plots in the cubic phase are nearly circular with secondary resonances near the origin. We find strong damping in tetragonal and orthorhombic phases. The phase shifts strongly but systematically in the cubic phase, while the phase shift in the tetragonal phase appears chaotic. No measurable phase shift occurs in the orthorhombic phase. Softening in the stability field of the cubic phase has been fitted to a Vogel–Fulcher equation $f(T) = A \exp(E/(T - T_{vf}))$. Both single crystals and ceramics present similar activation energies (~ 0.2 eV) and different freezing temperatures T_{vf} (90 and 146 K; Fig. 8). To test for phonon-driven precursor effects, we also tested for the expected power law dependence ($\Delta (C_{11} - C_{12}) \sim |T - T_c|^{-K}$) and found that no such pure soft-mode model applies for BaTiO$_3$ (Fig. 9).

FIG. 4. (Color online) Stack of RUS spectra of BaTiO$_3$ ceramics collected during heating/cooling from 693 to 293 K. The *y* axis is amplitude. The individual spectra have been displaced in proportion to the temperature at which they were collected, and the axis label is shown as temperature. Weak peaks, which do not vary with temperature, are from alumina rods of the high-temperature instrument. Resonance peaks completely disappear at $T_{CT} = 405$ K.
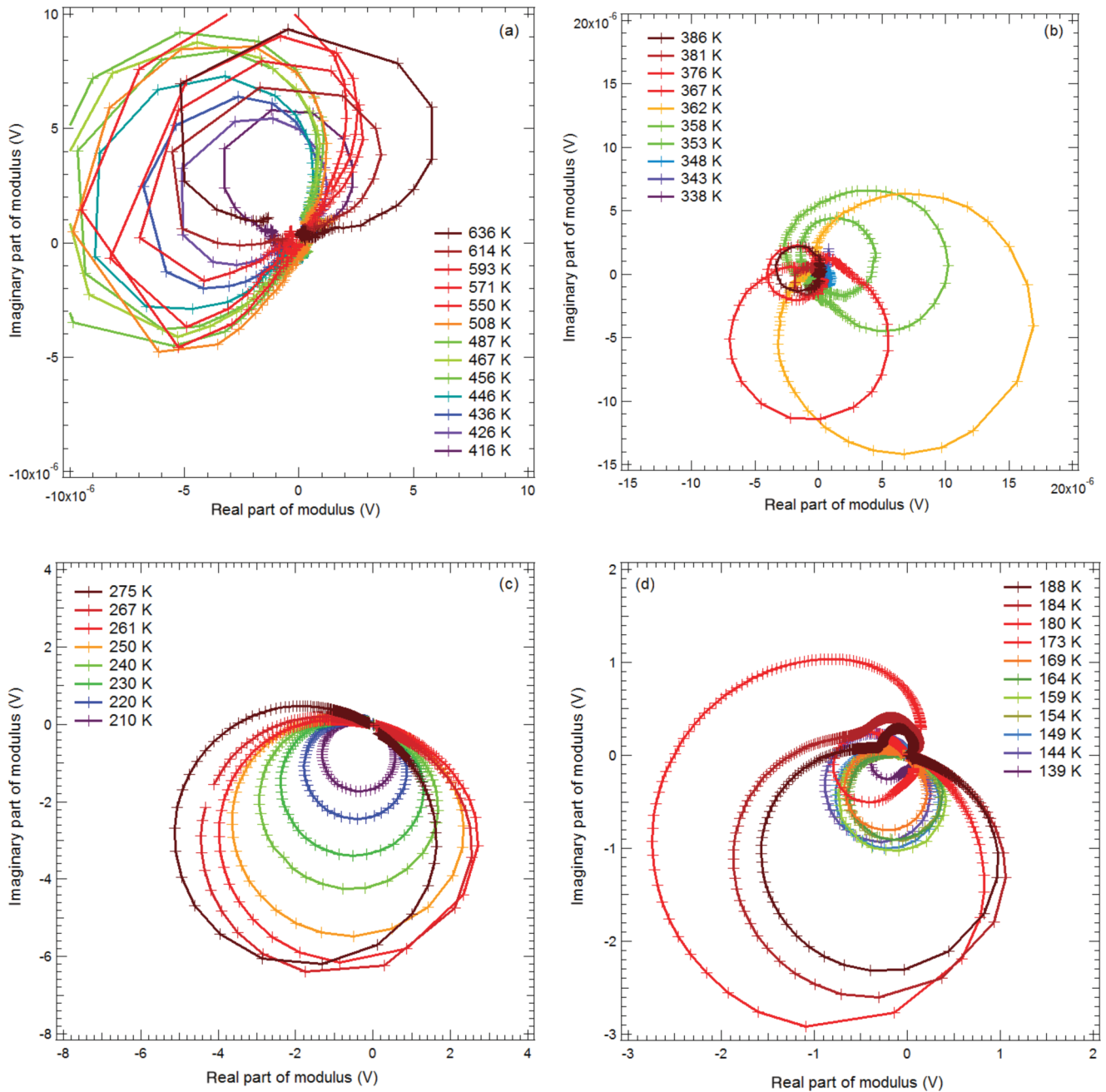
FIG. 6. (Color online) Nyquist diagrams for a single crystal of BaTiO$_3$ in the (a) cubic (265 kHz), (b) tetragonal (265 kHz), (c) orthorhombic (112 kHz), and (d) rhombohedral (112 kHz) phases. All spectra were taken on heating.

V. DISCUSSION

We showed that precursor softening is not a (purely) displacive phenomenon in BaTiO$_3$. The experimentally determined softening of the elastic constants in the cubic phase is related to the weakening of $C_{11} - C_{12}$, which relates to o/d processes and, in turn, indicates the appearance of PNRs (see Ref. 1 for comparison with Brillouin scattering data, which identified the soft modulus as C_{11}). The PNRs are either soft themselves or generate the softening by interfacial slip-slide mechanisms. The latter mechanism can be excluded because the softening of the effective elastic modulus $\Delta (C_{11} - C_{12})$ is not correlated with increased dissipation, which we would expect in a slip-slide mechanism.

The temperature evolution of the RUS frequency for the ceramic (Fig. 2) shows two tendencies. First, we find a weak hardening of the sample with decreasing temperature above ∼600 K. This tendency is overcompensated by the appearance of PNRs below the "Burns temperature T_B". This temperature is not clearly defined;[42] we can locate T_B below the maximum of the frequency at 586 K. The onset of the curvature in Fig. 8 shows the deviation from the exponential softening towards a weaker temperature dependence near 560 K, which we would then identify with the onset of the nucleation of PNRs in the single crystal. Therefore, $T_B = 560$ K would be a little higher than the value previously found by acoustic emission measurements carried out on a single crystal of BaTiO$_3$:
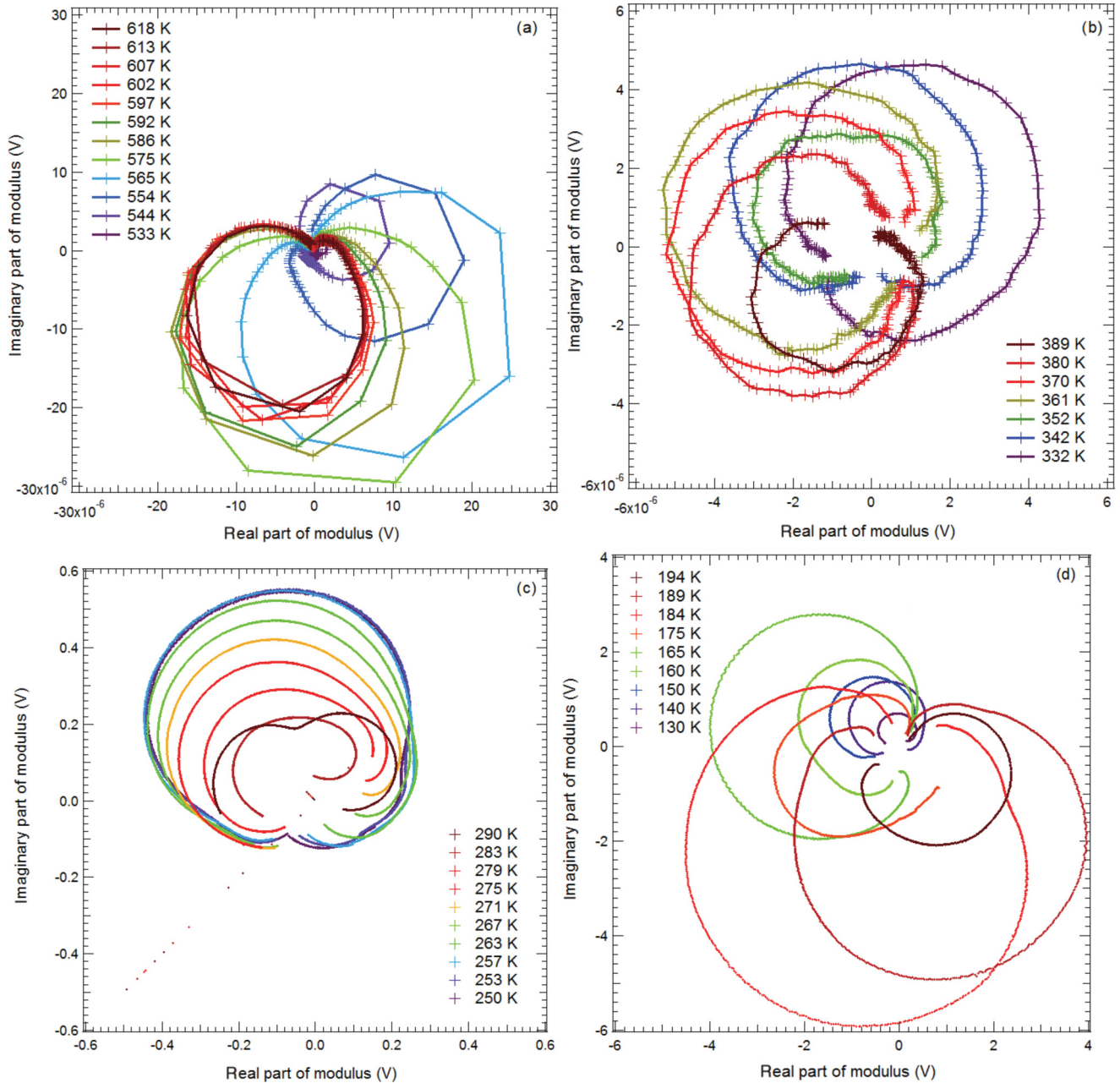
FIG. 7. (Color online) Nyquist diagram of BaTiO$_3$ ceramics in the (a) cubic (815 kHz), (b) tetragonal (923 kHz), (c) orthorhombic (770 kHz), and (d) rhombohedral (994 kHz) phases. All spectra were taken on heating.

$T_B = 553$ K.[42] Lowering the temperature further, we find the PNRs to soften the elastic response further until the phase transition near 405 K destroys the cubic symmetry. The softening is not related to phonon soft modes, which would lead to temperature dependences in the form of power laws.[35] Instead, we find an intrinsic temperature dependence in the form of Vogel–Fulcher dynamics. The activation energy is ∼0.2 eV, which is comparable with previous results in LaAlO$_3$.[31] Vogel–Fulcher dynamics are indicative of glassy systems, and it makes sense to envisage the network of the PNRs as a glassy substructure, which is only weakly coupled with the soft modes. Our results confirm the observations in Ref. 1 and match the functional form of the temperature dependence.

The PNRs in the ceramics are very similar to those of the single crystal. Our data seem to indicate that the onset temperature is lower (550 K) than in the single crystal (560 K) and also low compared with the temperature of the maximum value of $C_{11} - C_{12}$ (586 K; Fig. 9).

The temperature dependence of the phase factor is similar for both samples. We find rotations of the complex response function in the Nyquist plots in the cubic phase, which is indicative of a multitude of competing resonance modes with different phases. This can be understood if we consider large changes of the microstructure, which may be directly related to the PNRs and their effect on the dynamic elastic response of the sample. The nucleation of the PNRs in various parts of the
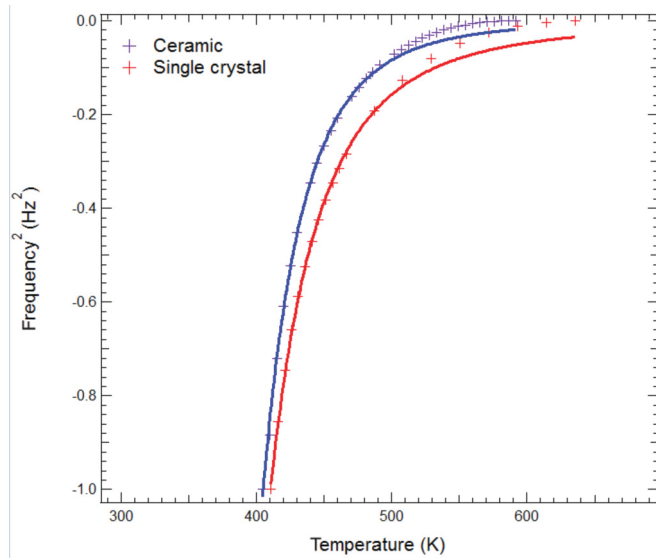
FIG. 8. (Color online) Precursor softening and Vogel–Fulcher analysis for a single crystal and a ceramic sample. The measured RUS frequencies follow a thermally activated precursor softening $\sim\exp[E/(T - T_{\mathrm{VF}})]$ typical for multivalley structures with glassy microstructures and order/disorder behavior.

samples could generate these phase rotations well. Rotations in the tetragonal phase show highly mobile twin boundaries, while nothing of this kind occurs in the orthorhombic phase. This phase contains a stable microstructure, probably due to mutual pinning of the various sets of twin boundaries. This pinning is much weaker in the rhombohedral phase, where some changes of the phase angle still occur.

The fundamental difference between the RUS spectra in single crystals and ceramics of BaTiO₃ relates to the damping of the resonance signal. The single crystal spectra show
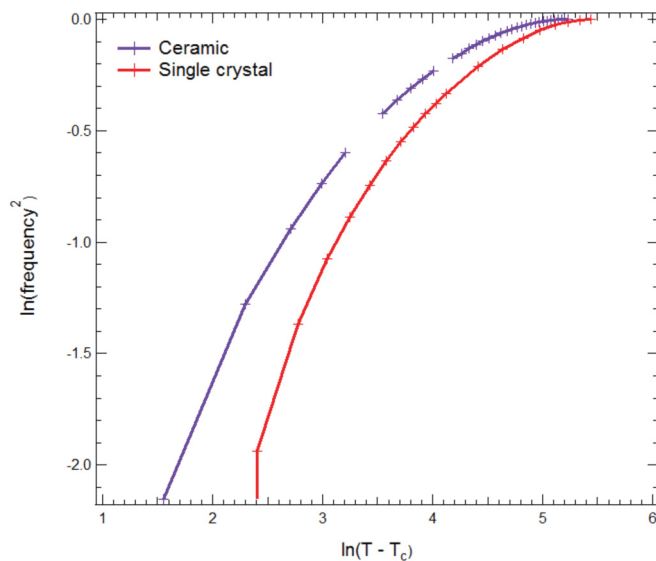

FIG. 9. (Color online) Precursor softening and power-law analysis for a single crystal and a ceramic sample. This softening is typical for displacive systems. The strong deviation from the power law proves that the precursor effect in BaTiO₃ is not (purely) phonon driven.

low values of Q^{-1} (<0.002) in the cubic and tetragonal phases. At temperatures near the transition points, the damping increases, which is the common behavior for nucleating microstructures.[25] With decreasing temperature, the damping increases in the single crystal. This effect has been observed before in other materials and is attributed to freezing of the twin wall movements (e.g. Ref. [29]). While the single crystal shows this classic behavior, we find that the ceramic behaves very differently. The damping in the tetragonal and orthorhombic phases is much greater than in any of the single crystal phases ($Q^{-1} \approx 0.03$; Fig. [2]). Decreasing the temperature decreases the damping until it attains values comparable with the single crystal near 110 K. Here, Q^{-1} may still decrease at lower temperatures below the freezing values of the single crystal (0.02). The key difference between the single crystal and the ceramic is hence the strong damping of the RUS signal in the tetragonal phase and, to a lesser extent, in the orthorhombic phase of the ceramic while the damping in the rhombohedral and cubic phases is roughly the same in the ceramic and the single crystal. No domain freezing seems to occur in the ceramic, while this effect is clearly visible in the single crystal.

We now discuss the increased damping in the tetragonal phase by a factor ~30 compared with the cubic phase. As the damping does not increase in the cubic phase, we can exclude remaining PNRs in the tetragonal phase as dissipating objects. Another possibility is that friction in the movement of intersections between twin walls and a much-enlarged surface area in the ceramic leads to dissipation. This model can be ruled out for the following reasons. The surface strain of twin walls is only weakly sensitive to the symmetry of the ferroelastic phase.[43] The high damping disappears gradually in the orthorhombic phase, while the twinning is likely to remain constant, and intersections between orthorhombic and rhombohedral twin walls and the grain surfaces are expected not to change with temperature. This leaves the structure of the tetragonal twins and their twin walls as temperature-dependent dissipators. Note, however, that, in RUS, the applied strain is very small ($\sim10^{-7}$),[31] which is much smaller than in the more commonly used DMA technique.[30,31] Friction in RUS is, hence, not related to large distance movement of twin boundaries but relates to local vibrations of twin walls and variations of the local wall structures.

We now explore how our RUS data are related to the dynamics of the polarization. For that, we decided to carry out molecular dynamics (MD) simulations for BaTiO₃ single crystals, employing the effective Hamiltonian approach of Ref. [44].

The effective Hamiltonian has been constructed to model (Ba,Sr)TiO₃ (BST) compounds for any Ba composition. The total energy E_{tot} given in this scheme has the form:

$$E_{\mathrm{tot}} = E_{\mathrm{VCA}}(\{\boldsymbol{u}_i\},\{\boldsymbol{v}_i\},\{\eta_H\}) + E_{\mathrm{loc}}(\{\boldsymbol{u}_i\},\{\boldsymbol{v}_i\},\{\eta_{\mathrm{loc}}\},\{\sigma_j\}),$$

where $\boldsymbol{u}_i$ denotes the local soft mode centered at the Ti atom of the unit cell i (i.e. $\boldsymbol{u}_i$ is directly proportional to the electric dipole of that cell); $\boldsymbol{v}_i$ are the dimensionless displacement variables of the cell corners and are used to calculate inhomogeneous strain tensor components for each cell i; $\{\eta_H\}$ is the homogeneous strain tensor, which allows the simulation supercell to vary in size and shape;[45] σ_j

characterizes the atomic configuration, with $\sigma_j = +1$ or -1, corresponding to the presence of a Ba or Sr atom, respectively, at the A-lattice site j; and $\{\eta_{loc}\}$ represents the local strain resulting from the difference in ionic size between Ba and Sr atoms,[44] which is relatively large ($\sim$2%). Here, E_{VCA} gathers the energy terms solely involving the local soft mode, strain, and their mutual couplings resulting from the application of the virtual crystal approximation (VCA)[46,47] to model $(Ba_{0.5}Sr_{0.5})TiO_3$ solid solutions. Also, E_{loc} can be thought of as a perturbative term due to the fact that BST systems possess real Ba and Sr atoms on the A-sites rather than virtual, composition-dependent atoms.

Previous Monte Carlo (MC) simulations performed for $BaTiO_3$ using this effective Hamiltonian scheme gave the exact ferroelectric (FE) phase transition sequence.[44] Furthermore, spectroscopic predictions from MD simulations of $BaTiO_3$ substantiated the observed central mode (CM) in THz spectroscopic measurements.[48,49]

Here, MD simulations were performed on a $12 \times 12 \times 12$ supercell of $BaTiO_3$ as follows: The system was equilibrated at a temperature of interest by running 100 000 MD steps of NPT (canonical ensemble) simulations, with each time step being 0.5 fs. Then the system was equilibrated at constant energy by conducting 40 000 MD steps of NVE (microcanonical ensemble) simulations. A subsequent 16 210 000 NVE steps were performed to obtain time-dependent properties of the investigated systems. These simulations predicted FE transition temperatures of 380, 285, and 230 K for $Pm\bar{3}m$ to $P4mm$, $P4mm$ to $Amm2$, and $Amm2$ to $R3m$, respectively, in good agreement with reported data[50,51] and current RUS observations. The complex dielectric response $\varepsilon(\omega)$ was then computed from the MD output using the approach of Refs. [49], [52–55]:

$$\varepsilon_{\alpha\beta}(\upsilon) - 1 = \frac{1}{\varepsilon_0 V k_B T}\left[\int_0^{t_s} \frac{\langle d_\alpha(t) d_\beta(t)\rangle}{t_S} dt + i2\pi\upsilon \int_0^\infty \langle d_\alpha(t) d_\beta(0)\rangle_\theta^{-i2\pi\upsilon t} dt \right],$$

where υ is the frequency; α, β are Cartesian components; V is the volume; T is the temperature; $d(t)$ is the dipole moment at time t, and angle brackets indicate thermal average. Peaks of complex dielectric response thus derived were then fitted using classical damped harmonic oscillators (DHO) of the form $\varepsilon(\upsilon) = S\upsilon_r^2/(\upsilon_r^2 - \upsilon^2 + i\gamma\upsilon)$, where υ_r, γ, and S are the resonant frequency, damping constant, and the dielectric strength, respectively, of the corresponding mode.

Figure 10 shows the highest and lowest resonant frequencies found in the simulations at each investigated temperature down to 240 K (i.e. just above the orthorhombic-to-rhombohedral transition). The lowest frequency corresponds to the central mode (CM), while the highest frequency is the soft mode (SM) in the cubic phase, while being the A_1 component of that soft mode in the tetragonal and orthorhombic phases. Consistent with Ref. [49], a central mode appears in the cubic phase for temperatures below 700 K. We postulate that the fact that the frequency of the central mode does not follow the same temperature dependency as the resonant frequency of the soft mode is related to the temperature dependency of the RUS phase factor.
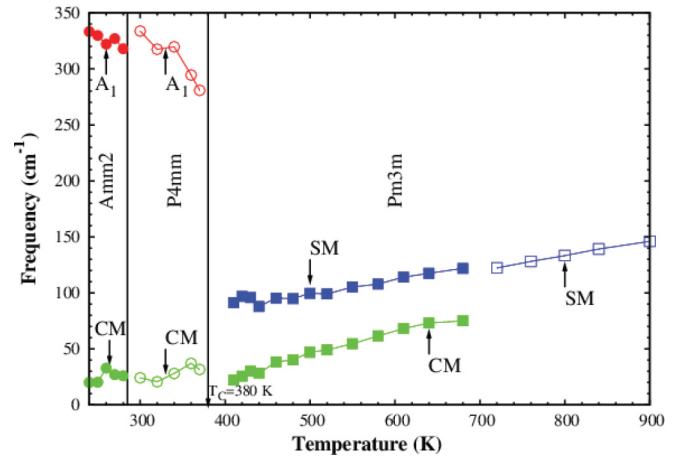

FIG. 10. (Color online) Temperature dependence of lowest and highest resonant frequencies, as obtained using DHO fittings of the MD dielectric spectra of $BaTiO_3$. The lowest resonant frequency corresponds to the central mode (green), while the highest frequency corresponds to the soft mode (blue) in cubic ($Pm\bar{3}m$) phase and the A_1 mode (red) in ferroelectric phases. Vertical lines correspond to phase transition temperatures.

As a matter of fact, the central mode reflects a flipping between different orientations of the Ti off-centering,[48] and hence a change of microstructure (or its local precursors) corresponds with our experimental RUS observations. Similarly, the fact that the predicted frequency of the A_1 component of the soft mode is strongly temperature dependent in the tetragonal phase, while that of the CM is not, is consistent with the strong temperature dependence of the RUS phase factor observed for the tetragonal phase. In the same manner, the simulations indicate that the resonant frequencies of the A_1 component of the soft mode and of the CM are nearly insensitive to the temperature in the orthorhombic phase, which bears resemblance with the observed constant RUS phase factor in this phase.

Several scenarios can be invoked to explain the large increase of the wall-related damping in ceramic $BaTiO_3$. First, it is possible that the chemical composition of the twin boundaries at room temperature is different for the ceramic and the single crystal. It is possible that the ceramic samples have a different oxygen concentration inside the twin walls from the bulk, which would increase the dissipation of any local movement. This possibility was already evoked in Refs. [28] and [29]; oxygen deficiencies inside domain walls were observed in other perovskite structures (e.g. Ref. [20]).

In addition, or alternatively, we may consider that domain walls are structurally different in the ceramic and the single crystal. A first indication that this proposition is reasonable stems from the observation that the thickness of the twin walls is some 2 nm in single crystals, while ceramics may have much narrower walls.[7] Computer simulations of the evolution of such thin walls under external strain[17] have shown that the main dissipation mechanism is related to the movement of kinks inside the walls and the nucleation of side arms of secondary walls from the original twin wall. In no case was a large-scale lateral movement of a twin wall observed which would be likely only for large (DMA-type) strains. The

movement of kinks and nucleation of additional walls have very little effect on the RUS resonance frequency. They were found to increase the damping very significantly, however, so that this mechanism would indeed explain our observations. Additional indirect support for this idea stems from the observation in Ref. 49, where dielectric measurements and simulations in the cubic phase of BaTiO$_3$ using a simple "toy" Hamiltonian illustrated that the dynamic excitations show two low-energy branches. These are the classic soft mode and a low-frequency excitation, which reflects the double-well properties of the Ti positions and their flips between these wells ($\sim$central peak). The consequence of such coupled systems is a heterogeneous ground state where the interfacial properties relate to strongly repulsive dynamical interactions (either flip or small displacement inside an energy minimum) and hence positive order parameter coupling ($\lambda > 0$ in Ref. 56). These conditions were shown to generate chiral twin walls,[56] which depend sensitively on the boundary conditions of the BaTiO$_3$ grains. This phenomenon may hence explain the observed difference between RUS signals of the single crystal and the ceramic sample.

The second difference originates from the precursor softening. For both samples, we find that the softening is not an intrinsic soft-mode behavior but relates to the coupling between the soft mode and the local double-well potentials. A general theory and simulations of dipolar correlations were published in Ref. 57. They predict that the temporary structures (snapshots at a timescale slightly longer than the phonon time) consist of a tweedlike pattern. The activation energy is given by the depth of the double-well potential and is the same for single crystals and ceramics. The Vogel–Fulcher temperature depends on the topological pathways for relaxations in such structures and depends on the finer details of the "glassy" tweed structures. Our results suggest that the ceramic samples have a lower Vogel–Fulcher temperature than the single crystal. Here, T_{VF} coincides roughly with the phase transition temperature in single crystals but is deeply inside the tetragonal phase in ceramics. This reduction in T_{VF} in the ceramic sample suggests that glassy relaxations continue more strongly in the tetragonal phase of the ceramic than the single crystal. This idea that hopping of Ti as the dominant order/disorder process is strong in the cubic phase but also persists in the tetragonal phase agreed with the findings in Ref. 48, where a strong central peak was still observed in the tetragonal phase.

In this paper, we used the term "PNR" in its broadest meaning; our experimental results and simulations clearly show that the precursor effect is dynamic and that elastic softening is an intrinsic property of the structure. Here, the recent discussion of Hlinka[58] becomes important. Our PNRs can well be seen as structural states inside a dynamic tweed structure and have little to do with well-defined, static clusters in a nonpolar matrix.

*Corresponding author: ekhard@esc.cam.ac.uk

[1]J. H. Ko, T. H. Kim, K. Roleder, D. Rytz, and S. Kojima, Phys. Rev. B **84**, 094123 (2011); T. H. Kim and J. H Ko, J. Korean Phys. Soc. **59**, 2575 (2011).

[2]S. Wada, T. Suzuki, M. Osada, M. Kakihana, and T. Noma, Jpn. J. Appl. Phys. **37**, 5385 (1998).

[3]R. Coes, M. Lambert, and A. Gunier, Solid State Commun. **6**, 715 (1968).

[4]K. Namikawa, M. Kishimoto, K. Nasu, E. Matsushita, R. Z. Tai, K. Sukegawa, H. Yamatani, H. Hasegawa, M. Nishikino, M. Tanaka, and K. Nagashima, Phys. Rev. Lett. **103**, 197401 (2009).

[5]K. Wieczorek, A. Ziebinska, Z. Ujma, K. Szot, M. Gorney, I. Franke, J. Koperski, A. Soszynski, and K. Roleder, Ferroelectrics **336**, 61 (2006).

[6]J. P. Sokoloff, L. L. Chase, and D. Rytz, Phys. Rev. B **38**, 597 (1988).

[7]J. H. Ko, S. Kojima, T. Y. Koo, J. H. Jung, C. J. Won, and N. J. Hur, Appl. Phys. Lett. **93**, 102905 (2008).

[8]F. Jona and G. Shirane, *Ferroelectric Crystals* (Permagon Press, Oxford, London, New York, 1962).

[9]S. Wada, K. Yako, H. Kakemoto, T. Tsurumi, and T. Kiguchi, J. Appl. Phys. **98**, 014109 (2005); M. Zgonik, P. Bernasconi, M. Duelli, R. Schlesser, P. Gunter, M. H. Garrett, D. Rytz, Y. Zhu, and X. Wu, Phys. Rev. B **50**, 5941 (1994).

[10]D. Damjanovic, M. Budinir, and M. Davis, J. Mater. Sci. **41**, 65 (2006).

[11]S. Wada and T. Tsurumi, British Ceramic Transactions **103**, 93 (2003).

[12]M. Davis, M. Budimir, M. Damjanovic, and N. Setter, J. Appl. Phys. **101**, 054112 (2007).

[13]R. Ahluwalia, T. Lookman, A. Saxena, and W. W. Cao, Phys. Rev. B **72**, 014112 (2005).

[14]Z. Valdez-Nava, C. Tenailleau, S. Guillemet-Fritsch, N. El Horr, T. Lebay, P. Dufour, B. Durand, and J. Y. Chane-Ching, J. Phys. Chem. Solids **72**, 17 (2011).

[15]Y. L. Zhu, S. J. Zheng, D. Chen, and X. L. Ma, Thin Solid Films **518**, 3669 (2010).

[16]Y. C. Wu, H. Y. Lu, D. E. McCauley, and M. S. H. Chu, J. Am. Ceram. Soc. **89**, 2702 (2006); E. Hamada, W. S. Cho, and K. Takayanagi, Philos. Mag. A **77**, 1301 (1998).

[17]E. K. H. Salje, X. Ding, Z. Zhao, T. Lookman, and A. Saxena, Phys. Rev. B **83**, 104109 (2011); E. K. H. Salje, X. Ding, Z. Zhao, and T. Lookman, Appl. Phys. Lett. **100**, 22905 (2012).

[18]E. K. H. Salje, Chem. Phys. Chem. **11**, 940 (2010).

[19] E. Salje and H. Zhang, Phase Transitions **82**, 452 (2009).

[20] A. Aird and E. K. H. Salje, J. Phys.: Condens. Matter **10**, L377 (1998); Y. Kim, M. Alexe, and E. K. H. Salje, Appl. Phys. Lett. **96**, 032904 (2010).

[21] J. Seidel, P. Maksymovych, Y. Batra, A. Katan, S. Y. Yang, Q. He, A. P. Baddorf, S. V. Kalinin, C. H. Yang, J. C. Yang, Y. H. Chu, E. K. H. Salje, H. Wormeester, M. Salmeron, and R. Ramesh, Phys. Rev. Lett. **105**, 197603 (2010).

[22] D. Meier, J. Seidel, A. Cano, K. Delaney, Y. Kumagai, M. Mostovoy, N. A. Spaldin, R. Ramesh, and M. Fiebig, Nat. Mater. **11**, 284 (2012).

[23] Y. P. Chiu, Y. T. Chen, B. C. Huang, M. C. Shih, J. C. Yang, Q. He, C. W. Liang, J. Seidel, J. C. Chen, R. Ramesh, and Y. H. Chu, Adv. Mater. **23**, 1530 (2011).

[24] S. Van Aert, S. Turner, R. Delville, D. Schryvers, G. Van Tendeloo, and E. K. H. Salje, Adv. Mater. **24**, 523 (2012); L. Goncalves-Ferreira, S. A. T. Redfern, E. Artacho, and E. K. H. Salje, Phys. Rev. Lett. **101**, 097602 (2008); M. Calleja, M. T. Dove, and E. K. H. Salje, J. Phys.: Condens. Matter **15**, 2301 (2003); **13**, 9445 (2001); M. A. Carpenter, A. Buckley, P. A. Taylor, and T. W. Darling, *ibid.* **22**, 035405 (2010); M. A. Carpenter and Z. Zhang, Geophys. J. Intern. **186**, 279 (2011).

[25] D. Shilo, H. Drezner, and A. Dorogoy, Phys. Rev. Lett. **100**, 035505 (2008).

[26] A. Gurevich and E. A. Pashitskii, Phys. Rev. B **57**, 13878 (1998).

[27] E. K. H. Salje, H. Zhang, H. Idrissi, D. Schryvers, M. A. Carpenter, X. Moya, and A. Planes, Phys. Rev. B **80**, 134114 (2009).

[28] V. Stepkova, P. Marton, and J. Hlinka, J. Phys.: Condens. Matter **24**, 212201 (2012); P. Marton, I. Rychetsky, and J. Hlinka, Phys. Rev. B **81**, 144125 (2010).

[29] J. Hlinka, P. Ondreikovic, and P. Marton, Nanotechnology **20**, 105709 (2009).

[30] A. V. Kityk, W. Schranz, P. Sondergeld, D. Havlik, E. K. H. Salje, and J. F. Scott, Phys. Rev. B **61**, 946 (2000); W. Schranz, P. Sondergeld, A. V. Kityk, and E. K. H. Salje, *ibid.* **80**, 094110 (2009); R. J. Harrison, S. A. T. Redfern, A. Buckley, and E. K. H. Salje, J. Appl. Phys. **95**, 1706 (2004).

[31] A. Migliori and J. D. Maynard, Rev. Sci. Instrum. **76**, 121301 (2005); M. A. Carpenter, E. K. H. Salje, and C. J. Howard, Phys. Rev. B **85**, 224430 (2012); E. K. H. Salje and M. A. Carpenter, Appl. Phys. Lett. **99**, 051907 (2011); J. Phys.: Condens. Matter **23**, 112208 (2011).

[32] F. Kremer and A. Schonhals, *Broadband Dielectric Spectroscopy* (Springer, Berlin and Heidelberg, 2002).

[33] E. K. H. Salje, J. Koppensteiner, M. Reinecker, W. Schranz, and A. Planes, Appl. Phys. Lett. **95**, 231908 (2009).

[34] M. Landa, P. Sedlak, H. Seiner, L. Heller, L. Bicanove, P. Sittner, and V. Novak, Appl. Phys. A **96**, 557 (2009).

[35] M. A. Carpenter and E. K. H. Salje, Eur. J. Mineralogy **10**, 693 (1998).

[36] M. A. Carpenter, E. C. Wiltshire, C. J. Howard, R. I. Thomson, S. Turczynski, D. A. Pawlak, and T. Lukasiewicz, Phase Transitions **83**, 703 (2010); E. K. H. Salje and W. Schranz, Z. Kristallogr. **226**, 1 (2011).

[37] S. J. Martin, H. L. Bandey, R. W. Cernosek, A. R. Hillman, and M. J. Brown, Anal. Chem. **72**, 141 (2000).

[38] P. C. Y. Lee, N. H. Liu, and A. Ballato, IEEE Trans. Ultrason. Ferroelectr. Freq. Control **541**, 52 (2004).

[39] A. V. Boiko, V. M. Kulik, B. M. Seoudi, H. H. Chun, and I. Lee, Int. J. Solids Struct. **47**, 374 (2010).

[40] R. E. A. McKnight, M. A. Carpenter, T. W. Darling, A. Buckley, and P. A. Taylor, Am. Mineral. **92**, 1665 (2007); R. E. A. McKnight, T. Moxon, A. Buckley, P. A. Taylor, T. W. Darling, and M. A. Carpenter, J. Phys.: Condens. Matter **20**, 075229 (2008).

[41] G. Picht, H. Kungl, M. Baurer, and M. J. Hoffmann, Funct. Mater. Lett. **3**, 59 (2010).

[42] E. Dul'kin, J. Petzelt, S. Kamba, E. Mojaev, and M. Roth, Appl. Phys. Lett. **97**, 032903 (2010).

[43] J. Novak and E. K. H. Salje, J. Phys.: Condens. Matter **10**, L359 (1998).

[44] L. Walizer, S. Lisenkov, and L. Bellaiche, Phys. Rev. B **73**, 144105 (2006).

[45] W. Zhong, D. Vanderbilt, and K. M. Rabe, Phys. Rev. B **52**, 6301 (1995).

[46] L. Bellaiche and D. Vanderbilt, Phys. Rev. B **61**, 7877 (2000).

[47] N. J. Ramer and A. M. Rappe, J. Phys. Chem. Solids **61**, 317 (2000).

[48] J. Hlinka, T. Ostapchuk, D. Nuzhnyy, J. Petzelt, P. Kuzel, C. Kadlec, P. Vanek, I. Ponomareva, and L. Bellaiche, Phys. Rev. Lett. **101**, 167402 (2008).

[49] I. Ponomareva, L. Bellaiche, T. Ostapchuk, J. Hlinka, and J. Petzelt, Phys. Rev. B **77**, 012102 (2008).

[50] C. Menoret, J. M. Kiat, B. Dkhil, M. Dunlop, H. Dammak, and O. Hernandez, Phys. Rev. B **65**, 224104 (2002).

[51] V. V. Lemanov, E. P. Smirnova, P. P. Syrnikov, and E. A. Tarakanov, Phys. Rev. B **54**, 3151 (1996).

[52] J. M. Caillol, D. Levesque, and J. J. Weis, J. Chem. Phys. **85**, 6645 (1986).

[53] D. Wang, J. Weerasinghe, L. Bellaiche, and J. Hlinka, Phys. Rev. B **83**, 020301(R) (2011).

[54] I. Grinberg, Y. H. Shin, and A. M. Rappe, Phys. Rev. Lett. **103**, 197601 (2009).

[55] J. Weerasinghe, D. Wang, and L. Bellaiche, Phys. Rev. B **85**, 014301 (2012).

[56] S. Conti, S. Muller, A. Poliakovsky, and E. K. H. Salje, J. Phys.: Condens. Matter **23**, 142203 (2011).

[57] A. M. Bratkovski, A. M. Marais, V. Heine, and E. K. H. Salje, J. Phys.: Condens. Matter **6**, 3679 (1994); K. Parlinski, V. Heine, and E. K. H. Salje, *ibid.* **5**, 497 (1993).

[58] J. Hlinka, J. Adv. Dielectrics **2**, 1241006 (2012).